Leckie, R.M., Sigurdsson, H., Acton, G.D., and Draper, G. (Eds.), 2000
Proceedings of the Ocean Drilling Program, Scientific Results, Vol. 165

5. GRAIN SIZE OF MIOCENE VOLCANIC ASH LAYERS FROM SITES 998, 999, AND 1000: IMPLICATIONS FOR SOURCE AREAS AND DISPERSAL[1]

Steven Carey[2] and Haraldur Sigurdsson[2]

ABSTRACT

Crystal size measurements have been carried out on tephra fall layers of Miocene to Holocene age from Sites 998, 999, and 1000 in the western Caribbean Sea. Maximum crystal size is used as a proxy for the grain-size characteristics of the layers and an index of atmospheric dispersal from source eruptions. Crystal sizes range from 50 to 650 µm with the majority falling between 200 and 300 µm. All three sites exhibit a coarsening in the grain size of tephra layers with increasing age to the early Miocene that broadly correlates with an increase in the frequency of layers. Analysis of the present lower and upper level atmospheric circulation in the western Caribbean suggests that the layers were derived from source eruptions to the west of the sites somewhere in the Central American region. Minimum distances to these sources are on the order of 700 km. Crystal sizes in tephra layers at these distances are consistent with their derivation from energetic pyroclastic flow-forming eruptions that ejected tephra to stratospheric levels by large-scale ignimbrite- and Plinian-style plumes. Coarsening of the layers during the Miocene peak of explosive volcanism cannot be attributed to any major change in paleowind intensity and is taken to represent the occurrence of more energetic eruptions that were able to disperse tephra over larger areas.

INTRODUCTION

One of the major discoveries of Leg 165 drilling in the western Caribbean was the great abundance of volcanic ash layers interbedded with dominantly pelagic sediments (Sigurdsson, Leckie, Acton, et al., 1997). In total, more than 2000 ash layers from Sites 998, 999, 1000, and 1001 were identified during shipboard core description. Site 999 contained the most complete record of tephra deposition with excellent recovery of sediments spanning ~70 m.y. Most of the layers were produced by the fallout of ash from the atmosphere during large-scale explosive eruptions. They consist of abundant clear glass shards, crystals, lithics, and alteration products, such as smectitic clay. Most layers are several to tens of centimeters thick with sharp bases and bioturbated tops. However, some were deposited from sediment gravity flows, implying a more proximal source of material.

The presence of ash or tephra fall layers define two major peaks of explosive volcanism during the early to mid-Miocene and the mid- to late Eocene (Sigurdsson, Leckie, Acton, et al., 1997). It has been proposed that the source area for the Miocene tephra layers was an extensive Tertiary volcanic province that extended through Central America and produced large volumes of explosive volcanism, now preserved as voluminous ignimbrite deposits. The cumulative thickness of Miocene tephra layers in the western Caribbean sites also suggests that the main dispersal axis of tephra fallout was located somewhere near Site 999 in the Colombian Basin.

In general, the grain size and thickness of tephra fall layers are determined by a combination of prevailing wind strength, initial size range of tephra, and eruption column height (Carey, 1996). Thus, if the atmospheric circulation in an area is known, grain-size and thickness parameters can be used to infer the location and characteristics of the source eruptions. In this paper we present a study of the grain size of tephra layers from the major Miocene peak in explosive volcanism preserved at Sites 998, 999, and 1000. The work focuses on using crystal size as a parameter for evaluating the dispersal characteristics of individual tephra layers. Results of the work are integrated with existing information about the atmospheric circulation in the study area to evaluate the potential source areas of the layers and to make inferences about the nature of the source eruptions.

METHODS

Many of the tephra fall layers from Leg 165 sites have been altered to clay minerals or indurated by the process of cementation. It is not possible, therefore, to determine their overall grain-size characteristics. However, all the layers contain unaltered phenocrysts of feldspar, biotite, hornblende, or pyroxene. In this study we have used the size of the largest feldspar crystals as a measure of the grain-size characteristics of the layers and consequently, an indicator of the dispersal efficiency of the source eruption. The advantage of this approach is that it considers the settling behavior of grains with a uniform density and relatively simple shapes. In contrast, the more abundant, but often altered, glass shards have complex shapes that can significantly affect their settling rate in the atmosphere and make size comparisons between layers difficult (Wilson and Huang, 1979).

Tephra layers were selected randomly throughout the Miocene to Holocene sequences of Sites 998, 999, and 1000. Only samples from the base of the layers, where the grain size is typically largest, were used for the study. Grain mounts were prepared by treating the tephra samples with acetic acid, disaggregating them with an ultrasonic cleaner, and then sieving the sample to isolate the largest grain-size fraction. The 20 largest feldspar crystals in each slide were measured individually (longest and intermediate axes) using the National Institute of Health image analysis program. Crystal images were produced using a Zeiss Axioscopt petrographic microscope with a high-resolution charge coupled device video camera. Calibration of the video image allowed size measurements to be made with a precision of ±5 µm.

BACKGROUND

At Site 998, located on the Cayman Rise at a water depth of 3180 m (Fig. 1), we recovered a 638-m-thick, largely complete sedimentary section that extends from the lower Eocene to the Pleistocene. More than 500 tephra layers were identified at this site, interbedded with

[1]Leckie, R.M., Sigurdsson, H., Acton, G.D., and Draper, G. (Eds.), 2000. *Proc. ODP, Sci. Results,* 165: College Station, TX (Ocean Drilling Program).
[2]Graduate School of Oceanography, University of Rhode Island, Narragansett, RI 02882, U.S.A. scarey@gsosun1.gso.uri.edu

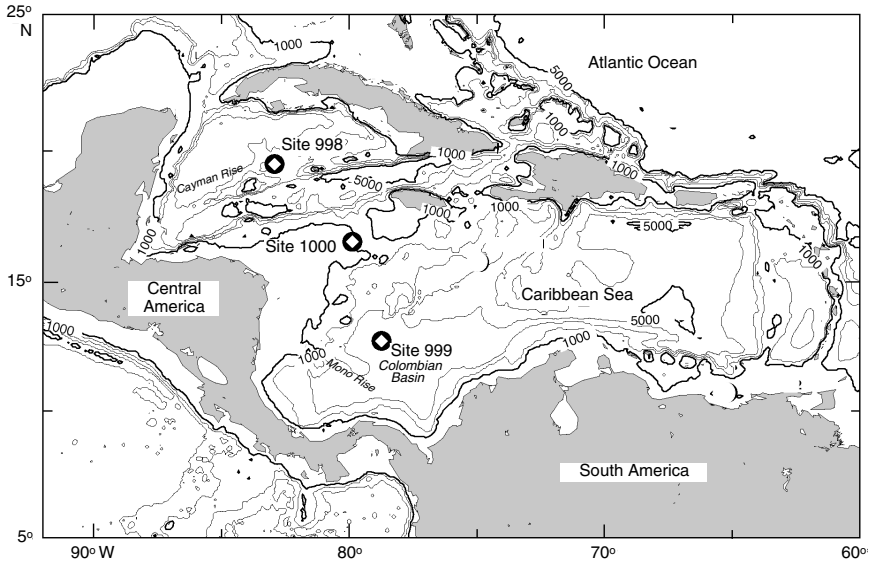

Figure 1. Map showing the major physiographic features of the Caribbean Sea and the location of the Leg 165 Sites 998, 999, and 1000. Contour intervals are in meters.

nannofossil and foraminiferal ooze, chalk, and limestone. Tephra fall layers were most abundant in the Miocene to Pleistocene sediments of lithologic Units I, II, and the upper parts of III. The Miocene fall layers contain abundant colorless glass shards of rhyolitic composition, with <10% crystals of plagioclase, quartz, biotite, hornblende, and clinopyroxene. In the older sections of Site 998 the abundance of ash turbidites increases dramatically with a prominent peak in the early Eocene (Shipboard Scientific Party, 1997a). These layers are typically altered and consist of a mixture of biogenic components (foraminifers and radiolarians) and volcaniclastic material (altered glass, plagioclase, quartz, biotite, Fe-Ti oxides, and igneous rock fragments).

Site 999 is located on a small rise at a water depth of 2827 m in the Colombian Basin ~150 km northeast of the Mono Rise (Fig. 1). It lies some 1000 m above the adjacent floor of the Colombian Basin and thus is outside of the influence of turbidite deposition from South America. It is also isolated by a saddle from redeposited sediment originating on the Hess Escarpment to the west. The relative stability of this site compared to nearby tectonic features such as the Hess Escarpment and Lower Nicaraguan Rise make this site ideal for a long-term record of tephra deposition.

An apparent complete and continuous sedimentary sequence of upper Maastrichtian to Pleistocene age was recovered in two holes that penetrated to 1066 meters below seafloor (mbsf). More than 1200 tephra fall layers were identified at this site, defining two prominent peaks in explosive volcanism during the middle to late Eocene and early to middle Miocene. Miocene to Pleistocene layers are interbedded with nannofossil clayey mixed sediment, clayey nannofossil mixed sediment, and clayey calcareous chalk of lithostratigraphic Units I, II, and III. They are similar in composition to the layers from Site 998, consisting of abundant rhyolitic glass shards, plagioclase, biotite, amphibole, rare quartz, and clinopyroxene. However, many of the layers are extensively altered with glass shards that are being converted to Mg-rich smectite. In addition, pyrite coating on glass shards is a common feature in many of the Miocene layers (Shipboard Scientific Party, 1997b). The extent of alteration does not appear to be systematic downcore. For example, many of the upper Miocene tephra fall layers are extensively altered, yet the majority of lower to middle-Miocene layers that constitute the major peak in ash abundance are relatively unaltered.

Site 1000 is located at a water depth of 916 m. This area is part of a series of carbonate shelves and isolated carbonate banks that form the Northern Nicaraguan Rise, extending from the coast of Honduras in the west to Jamaica in the east. An apparently complete sequence of late Miocene- to Holocene-age sediments was recovered by drilling to 696 mbsf. Tephra fall layers are interbedded with periplatform sediments and intervals of redeposited periplatform/pelagic and neritic carbonate sediments transported from the nearby shallow carbonate banks (Shipboard Scientific Party, 1997c). The majority of the tephra layers are extensively altered, although some contain colorless bubble-walled shards. Phenocryst phases include feldspar, biotite, and, more rarely, hornblende, Fe-Ti oxides, and quartz.

CRYSTAL SIZE MEASUREMENTS

Most studies of the grain size of tephra fall deposits in marine sediments have relied on a complete analysis of all components (Kennett, 1981). However, the extensive alteration of many of the Leg 165 tephra fall layers makes this approach impossible. In spite of the degradation of glass shards in the layers as they are converted to smectite, the majority of phenocrysts in the layers appear to remain relatively unaltered. Their size is thus a remnant proxy of the original size distribution of the entire layer. This, however, is based on the following assumptions: (1) the fragmented source mixture from an explosive eruption contains a subpopulation of crystals of sufficient size range to supply crystals that are aerodynamically equivalent to the largest juvenile (glassy) particles at distances >100 km downwind; and (2) the largest crystals are likely to be found at the base of a tephra fall layer. The first assumption is supported by many studies of terrestrial and marine tephra fall deposits in which phenocrysts are a ubiquitous component of distal deposits and are of a size that indicates aerodynamic equivalency in comparison to the less dense but larger juvenile components of the deposits (e.g., Carey and Sigurdsson, 1982; Cornell et al., 1983; Ninkovich et al., 1978). The second assumption is supported by observations of crystal-rich bases for many marine tephra fall deposits (Kennett, 1981) and the larger contrast in terminal settling velocity between glass shards and crystals when they are settling in water as compared to air (Cashman and Fiske, 1991). This difference in settling velocity would lead to an enhanced separation of the components during settling through the water column to the seafloor. Crystals would settle out ahead of aerodynamically equivalent glass shards and be concentrated at the base of layers.

An advantage to using crystal sizes as a proxy of grain size, and thus an index of dispersal, is that this component has a relatively constant density (~2.7 g/cm^3), and crystal shapes are more uniform (aspect ratio of ~0.6). Comparison of whole sample grain-size distribu-

tions can be problematic because the morphologies and compositions of the dominant glass shards can be quite variable and influence the settling velocity in a complex way (e.g., Wilson and Huang, 1979).

Site 998

Maximum feldspar sizes were measured in 26 tephra fall layers of early Miocene to Pleistocene age from Site 998 (Table 1). The long and intermediate axes were measured for each crystal. A typical set of measurements from a single sample is shown in Figure 2. The distributions are generally symmetrical, and from these the median and standard deviation of the measurements were calculated for each sample (Table 1). Median sizes of the longest crystal axis range from 50 to 300 µm, with the coarsest layers found in the lower to middle Miocene sites (Fig. 3). The majority of layers fall in a relatively narrow range, with median crystal sizes between 150 and 220 µm. There does not appear to be any correlation between the thickness of the layers and the maximum crystal sizes (Fig. 4). This result is somewhat surprising because it might be expected that thicker layers would correspond to larger eruptions and that these would be able to disperse coarser particles over a greater area.

For the Miocene as a whole, the complete data set of crystal measurements were combined to calculate the average dispersal properties of the tephra fall layers (Fig. 5). The median of the maximum feldspar sizes for the Site 998 Miocene tephra layers is 190 µm.

Site 999

Site 999 contains the highest accumulation rate of volcanic ash and the most number of tephra layers in the western Caribbean sites. Feldspar size measurements were carried out on 36 tephra fall layers of Miocene to Pleistocene age (Table 2). The median size of the 20 largest crystals varies from ~100 to 350 µm. There is also a general correlation between the median size of the crystals and the ash accumulation rate at this site (Fig. 6). The coarsest layers are in the middle to upper lower Miocene, similar to the size variation observed at Site 998 (Fig. 3). This correlation may be an indicator of (1) more energetic eruptions during this period, (2) increased wind strength, or (3) a higher probability of sampling coarser layers within sequences with a higher number of tephra fall layers.

As with Site 998, there does not seem to be any correlation between tephra layer thickness and the size of the largest feldspar crystals at Site 999 (Fig. 7). The median size of the Miocene fall layers as a whole is virtually identical to that of Site 998, with a value of 190 µm (Fig. 8).

Site 1000

Site 1000 did not penetrate beyond the Miocene sediments ending in sediment with an age of ~20 Ma. Feldspar measurements were carried out on 19 tephra fall layers (Table 3). This site exhibits the largest variation in median size of the 20 largest crystals, ranging from ~150 to ~600 µm. The median size is well correlated to the ash accumulation rate at this site, with the coarsest layers found to be in the upper lower Miocene (Fig. 9).

In contrast to Sites 998 and 999, there does appear to be some correlation between the median size of the largest feldspar crystals and the thickness of the tephra fall layers (Fig. 10). This site does, however, have a greater range in tephra fall thicknesses than Sites 998 and 999, with one layer up to 55 cm thick. The median size of the Miocene fall layers as a whole is slightly coarser than those at Sites 998 and 999, with a value of 260 µm (Fig. 11).

TRANSPORT OF TEPHRA IN THE WESTERN CARIBBEAN

Large-scale explosive eruptions can disperse tephra over large areas of the Earth's surface by injecting particles to high levels in the atmosphere in convective plumes (Sparks et al., 1997). The extent and direction of dispersal is a function of (1) eruption column height, (2) direction and intensity of the prevailing winds, and (3) size distribution of tephra from the source eruption. In order to evaluate potential source volcanoes for tephra fall deposits in a certain area, it is necessary to know the regional wind patterns at various elevations in the atmosphere. The western Caribbean area is characterized by a surface

Table 1. Feldspar size measurements of tephra fall layers, Site 998.

Core, section	Layer (cm) Top	Base	Thickness	Age (Ma)	Size (µm) Median	Average	Standard deviation	Maximum	Minimum
165-998A-									
3H-4	18	30	12.0	0.9	195	203	38	345	157
13H-3	18	33	15.0	7.6	219	226	35	320	184
13H-5	106	124	18.0	7.8	202	206	34	277	154
14H-6	0	21	21.0	8.7	181	181	36	257	127
16H-6	73	83	10.0	10.0	213	218	21	264	187
17H-4	119	129	10.0	10.7	219	223	41	328	157
20X-1	132.5	135	2.5	11.9	215	210	32	267	153
20X-2	3	14	11.0	14.0	205	215	41	309	145
20X-2	73	77	4.0	14.7	150	150	21	189	109
21X-1	125	132	7.0	15.1	198	199	32	267	144
21X-3	45	52	7.0	15.5	198	199	32	267	144
21X-4	60	80	20.0	15.6	305	309	46	459	259
23X-4	77	81	4.0	16.6	162	176	58	386	100
23X-5	36	50	14.0	16.7	150	156	24	217	132
24X-1	91	99	8.0	17.0	167	168	26	229	133
25X-1	90	108	18.0	17.5	47	52	22	108	24
25X-2	90	106	16.0	17.6	139	148	32	213	100
27X-1	115	121	6.0	18.8	288	294	45	389	195
27X-2	78	85	7.0	19.1	218	225	28	311	196
27X-3	21	22	1.0	19.2	165	167	19	200	135
27X-4	0	14	14.0	19.0	157	159	24	205	116
28X-1	100	115	15.0	22.1	229	223	37	277	155
28X-3	97	103	6.0	21.6	192	196	25	253	155
29X-3	68	70	2.0	20.1	298	318	80	551	232
36X-2	81	87	6.0	23.8	147	143	25	176	80
37X-1	140	148	8.0	24.5	175	175	22	223	146

Notes: Minimum size is of the 20 smallest feldspar crystals. All other measurements are of the 20 largest feldspar crystals. All measurements taken along the long axis.

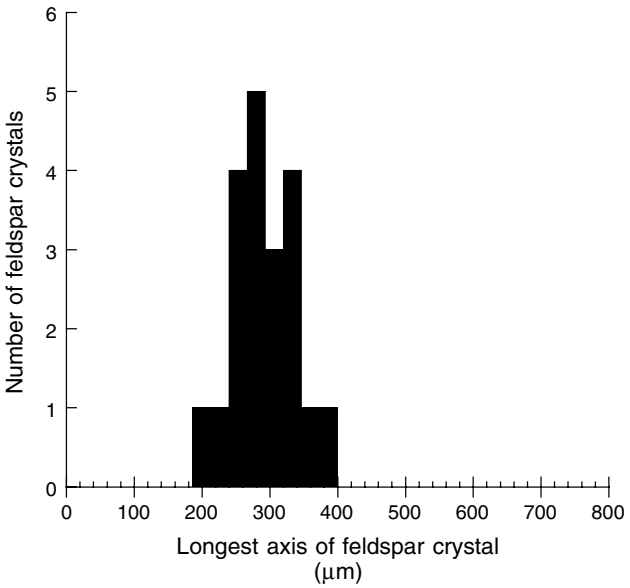

Figure 2. Distribution of long-axis measurements of feldspar crystals in a tephra fall layer from Site 998. Total number of measurements = 20.

flow that is dominated by the trade winds that blow from east to west (Fig. 12). However, at higher elevations there are significant changes in both the magnitude and direction of the prevailing winds. For example, at the 250 millibar level (~11 km elevation) the prevailing winds are switched by 180°, blowing from the west to the east (Fig. 13). Furthermore, the wind velocities at this altitude are two to three times as strong as the surface trade winds. At higher elevations (>20 km) the winds shift direction once again to a more east-southeasterly direction.

The vertical variations in wind intensity and direction are also complicated by a seasonal component. This can be seen from detailed records collected at Guatemala City, Guatemala, located at a latitude that is representative of the atmospheric circulation in the western Caribbean area (Fig. 14). Strong westerly winds in the lower stratosphere are most pronounced in winter and spring, but become more subdued in the summer and fall. As these winds decrease there is a strengthening of upper level winds >20 km height (Fig. 14).

Transport of tephra in the western Caribbean is likely to be complicated because of the observed reversal in transport direction with altitude (Fig. 14). However, some generalizations can be made regarding the importance of transport at different levels. In order for a widespread tephra layer to be formed in deep-sea sediments, it is necessary to have a sufficiently large source eruption. The location of Sites 998, 999, and 1000 from the Miocene to present indicate that the closest possible source area (Central America) is at a distance of at least 700 km (Fig. 15). In order to form tephra fall layers of several to tens of centimeters in thickness at such distances would require eruptions of several tens to hundreds of cubic kilometers of magma (e.g., Ninkovich et al., 1978). Eruptions of this type invariably produce convective eruption columns that inject large quantities of tephra well into the stratosphere (Carey and Sigurdsson, 1989). The tops of such columns may reach altitudes of 40 km or more and spread out to form a giant mushroom-shaped plume. Fallout of particles in these plumes occurs primarily from the base of the expanding mushroom-shaped cap, which will be of the order of 20 km height (Carey and Sparks, 1986). Dispersal of fine-grained tephra will therefore take place at levels above the tropopause, and in the western Caribbean it is likely to be controlled by strong westerly winds for at least a significant part of the year. It is possible, however, that easterly transport of some material would also take place at higher and lower altitudes. This bidirectional transport mechanism is well illustrated by the dispersal of

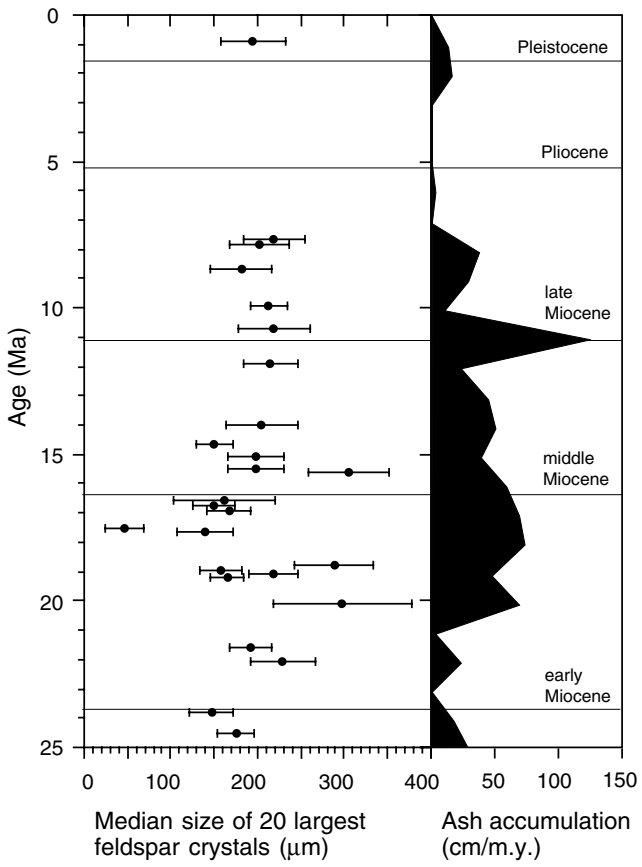

Figure 3. Variation in median size of the 20 largest feldspar crystals in tephra fall layers from Site 998 as a function of age (left). Also shown (right) is the record of total ash accumulation rate for Site 998 as a function of age (data from Sigurdsson, Leckie, Acton, et al., 1997).

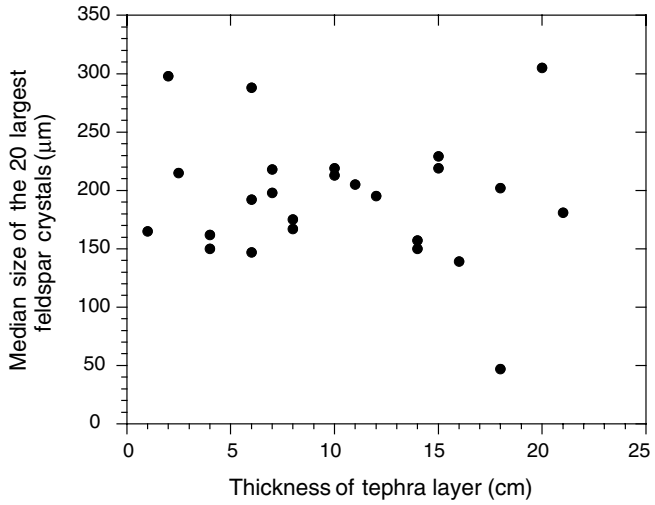

Figure 4. Variation in median size of the 20 largest feldspar crystals vs. thickness of tephra layer for Site 998.

tephra from a 84-ka eruption of Atitlan caldera in Guatemala (Drexler et al., 1980). The widespread Los Chocoyos tephra layer from this eruption is found in Pacific, Gulf of Mexico, and Caribbean sediments (Ledbetter, 1985; Drexler et al., 1980). Estimates of the total volume of the eruption are of the order of 200 km^3 of magma.

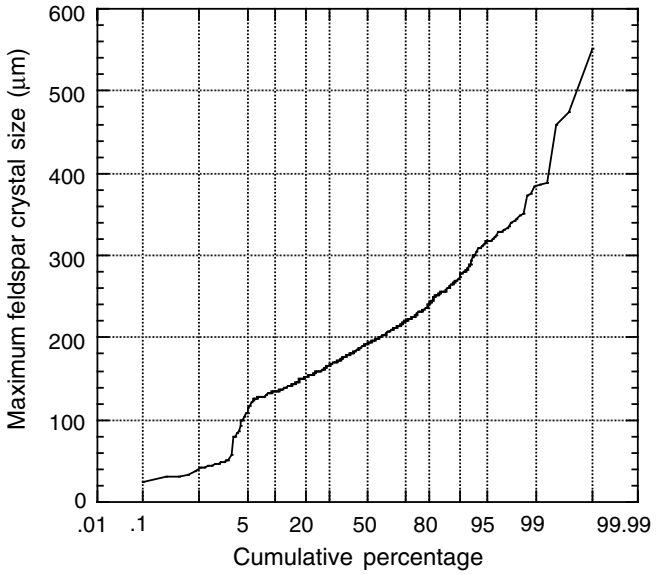

Figure 5. Cumulative percentage of maximum feldspar size in all measured Miocene tephra fall layers from Site 998.

SOURCE AREAS FOR WESTERN CARIBBEAN TEPHRA LAYERS

There are two potential sources of Miocene to Holocene volcanic ash in the western Caribbean: (1) Central America and southern Mexico, and (2) the Lesser Antilles volcanic arc to the east. In Central America there are two major Tertiary ignimbrite formations that extend from the Mexican border in the north through Guatemala, El Salvador, and Honduras, and into Nicaragua over a region that is more than 800 km in length and up to 300 km wide. The ignimbrite formations underlie upper Tertiary and Quaternary andesitic and basaltic andesite stratocones of the active Central American volcanic arc (Reynolds, 1980). However, the mid-Tertiary ignimbrite-bearing formations generally extend far east of the active arc. The major formations include silicic welded tuffs of the Chalatenango Formation in south-central Guatemala and El Salvador (Reynolds, 1987; Wiesemann, 1975), thick rhyolitic ignimbrites of the Padre Miguel Group in southeast Guatemala and Honduras (Reynolds, 1980), and the thick siliceous ignimbrites of the Coyol Group in Nicaragua (Ehrenborg, 1996). Reliable $^{40}Ar/^{39}Ar$ single crystal biotite ages for ignimbrites within the Coyol Group cluster from 12.3 to 18.4 Ma, defining an early–middle Miocene volcanic episode. Many of the formations are linked to caldera structures and have aggregate thicknesses of several hundred meters. Some of the co-ignimbrite tephra from eruptions of this ignimbrite province was transported into the Pacific where it was recovered off Guatemala during Deep Sea Drilling Project (DSDP) Leg 67 (Cadet et al., 1982a), and near the Middle America Trench off Mexico during DSDP Leg 66 (Cadet et al., 1982b).

The Lesser Antilles arc has been the site of explosive volcanism since at least the Eocene with the formation of tephra layers in marine sediments of the western equatorial Atlantic and eastern Caribbean (Natland, 1984; Sigurdsson et al., 1980; Sigurdsson and Carey, 1981). Drilling during Leg 78A of the DSDP in the Lesser Antilles forearc recovered siliceous volcanic ash layers with peak occurrences in the lower to middle Miocene, lower Pliocene, and upper Pleistocene (Natland, 1984). However, the main dispersal direction for the majority of fall layers is to the east into the Atlantic (e.g., Carey and Sigurdsson, 1980). This pattern appears to be a direct result of the importance of high-level transport where the strong winds blow from west to east. Minor transport of tephra has occurred to the east from the Lesser Antilles, but the amount has been insufficient to form discrete layers in the sediments beyond 100 km from the arc. The distribution of Quaternary tephra layers in the Lesser Antilles region thus provides an important analog for atmospheric transport processes occurring in the western Caribbean.

In view of the eastward dispersal of tephra from the Lesser Antilles and its great distance from the Leg 165 sites (>1800 km) we can rule out this area as the source of numerous tephra fall layers at Sites 998, 999, and 1000. It is, on the other hand, most likely that the source area of these layers is the widespread Tertiary volcanic province of Central America. This is supported by (1) the prevailing upper wind patterns and (2) the great abundance of Miocene-age ignimbrite deposits. Derivation of some layers from the Mexican ignimbrite province of the Sierra Madre Occidental is a possibility. However, the age of voluminous ignimbrite volcanism in the area (27–34 Ma; McDowell and Clabaugh, 1979) appears to be too old to explain the majority of Miocene layers. Further support for the Central American source area can be found by considering the measured feldspar sizes in relation to the likely distances from source eruptions.

NATURE OF SOURCE ERUPTIONS FOR WESTERN CARIBBEAN TEPHRA FALLS

Tephra fall deposits from large-scale explosive eruptions contain information about the source eruptions and the prevailing atmospheric conditions. Studies of marine- and land-based tephra fall deposits have demonstrated several systematic relationships that appear to apply universally to these types of layers. One of the more important is that both thickness and grain size decrease exponentially to distances of >1000 km from the source (Pyle, 1989; 1995). This type of decay reflects the underlying mechanism of sedimentation of particles from the upper umbrella regions of explosive eruption plumes (Sparks et al., 1991; Bursik et al., 1992).

The exponential decay of grain size and layer thickness can be used to place constraints on the size of the source eruptions. Based on arguments presented in the previous section, the atmospheric circulation in the Caribbean area favors a volcanic source that is located to the west of Sites 998, 999, and 1000. For the Miocene peak in explosive volcanism this source is likely to be the extensive Tertiary ignimbrite deposits that extend through Guatemala, Honduras, and Nicaragua. This province was at least 700 km from the Leg 165 sites, based on a reconstruction of the site locations during the Miocene (Fig. 15). Thus, the plate reconstructions place good constraints on the minimum distance from source with which to evaluate the size of the largest feldspar crystals.

Figure 16 presents maximum grain size and thickness relationships for three well-documented marine tephra fall deposits. The layers were produced by the 75-ka Toba eruption in Indonesia (Ninkovich et al., 1978), the 33-ka Campanian ignimbrite eruption in Italy (Cornell et al., 1983), and the Minoan eruption of Santorini ~1620 B.C. (Watkins et al., 1978). The data for these layers provide important recent analogs for the Miocene tephra fall layers in the western Caribbean. For example, the median size of the largest feldspar crystals in the Miocene tephra fall layers of Sites 998, 999, and 1000 are 190, 190, and 260 μm, respectively. If the minimum distance from source was 700 km, then these sizes are in line with eruptions of Campanian scale (Fig. 16). The Campanian eruption produced ~80 km^3 dense rock equivalent (DRE) of trachytic magma that was erupted as Plinian pumice fall and widespread pyroclastic flows (Barberi et al., 1978; Cornell et al., 1983). The eruption column is estimated to have been at least 44 km in height (Carey and Sigurdsson, 1989).

Because the western Caribbean sites lie at such great distances from potential sources (>700 km), the size of the feldspar crystals provide a robust signal of the size of the source eruptions. The data suggest very large magnitude source events (more than tens of cubic

Table 2. Feldspar size measurements of tephra fall layers, Site 999.

Core, section	Layer (cm) Top	Base	Thickness	Age (Ma)	Size (μm) Median	Average	Standard deviation	Maximum	Minimum
165-999A-									
6H-3	10	14	10	1.45	232	231	27	275	165
6H-5	10	12	10	1.57	150	155	13	183	138
17H-4	112	116	112	5.67	154	158	25	227	124
27X-2	145	150	145	9.01	290	295	39	400	237
34X-2	133	135	133	11.67	162	162	25	215	113
34X-3	45	54	45	11.69	194	204	46	312	146
36X-3	10	16	10	12.46	140	141	18	180	112
37X-6	46	50	46	13.06	284	281	48	367	206
39X-2	5	12	5	13.59	284	281	48	367	206
40X-1	54	60	54	13.95	116	116	15	152	92
40X-2	57	60	57	14.02	204	212	27	285	176
40X-4	82	85	82	14.16	280	279	33	350	220
42X-5	50	60	50	15.04	230	232	26	300	195
44X-2	73	79	73	15.68	219	214	38	297	139
47X-4	145	150	145	17.15	154	156	19	196	127
47X-5	104	116	104	17.2	174	179	28	260	132
48X-4	29	36	29	17.54	336	344	65	468	230
48X-6	42	43	42	17.69	336	337	59	484	245
49X-2	76	81	76	17.87	177	189	34	243	141
49X-3	50	54	50	17.93	266	280	46	414	226
49X-4	24	28	24	17.98	166	167	18	197	137
50X-1	70	79	70	18.25	194	203	34	275	146
50X-4	36	41	36	18.44	168	172	18	211	143
50X-4	103	110	103	18.47	202	212	48	356	155
51X-4	86	93	86	18.92	202	206	37	347	167
52X-1	72	77	72	19.16	110	118	29	194	87
52X-2	70	80	70	19.24	168	175	29	239	130
53X-4	140	145	140	19.89	184	181	23	222	134
54X-2	143	144	143	20.21	114	121	29	226	98
58X-5	58	62	58	21.87	112	115	29	190	79
165-999B-									
7R-3	53	59	53	24.65	112	115	29	190	79
7R-5	53	63	53	24.8	193	190	16	216	150
7R-CC	8	14.5	8	25.0	297	302	40	392	220
8R-1	51	57	51	25.0	156	159	12	190	143

Notes: Minimum size is of the 20 smallest feldspar crystals. All other measurements are of the 20 largest feldspar crystals. All measurements taken along the long axis.

kilometers in DRE magma volume) that were likely associated with the generation of voluminous ignimbrites and caldera formations. Much of the widespread fallout was probably derived from large-scale co-ignimbrite plumes that were generated from the tops of pyroclastic flows (e.g., Woods and Wohletz, 1991; Sparks and Huang, 1980). The abundance of thick ignimbrites in the Central American Tertiary volcanic province supports this interpretation.

DISCUSSION

The large-scale atmospheric circulation in the Caribbean area coupled with the abundance of Miocene silicic ignimbrites in Central America provide strong evidence that the source of the western Caribbean tephra fall layers was to the west of the Leg 165 sites during the Miocene to Holocene. Giant co-ignimbrite plumes generated from pyroclastic flow-generating eruptions injected tephra to stratospheric levels with subsequent dispersal both to the east and west of the Tertiary ignimbrite province. Many of the eruptions were likely to be similar to or larger than the great Campanian ignimbrite eruption in Italy that ejected 80 km^3 of magma. The crystal size data from Sites 998, 999, and 1000 also indicate a significant coarsening of the tephra at ~18 Ma, or coincident with the Miocene peak in ash accumulation rate (Figs. 3, 6, 9). This coarsening could be attributed to (1) the increased probability of sampling coarser layers in intervals that contain a higher number of tephra layers, (2) a strengthening of the winds that were dispersing material from a range of eruptions that remained of equal size over time, or (3) a period of more energetic eruptions that were dispersed over a larger area because of higher eruption column heights.

First, we consider the influence of sampling frequency. Tephra layers were selected randomly throughout the sequences and the frequency of sampling ranges from 1 layer/m.y. to a maximum of 6 layers/m.y. There does not appear to a be a strong correlation between the sampling frequency and the maximum crystal size found within a 1-m.y. interval (Fig. 17). There is a slight tendency for the coarsest layers at any given site to be found within the interval with the most layers, but there are many instances of relatively coarse layers being sampled in intervals where only one layer was selected. We feel, therefore, that sampling frequency alone cannot account for the significant increase in grain size found in layers near the peak in ash accumulations at Sites 998, 999, and 1000.

The next possibility to be considered is whether the coarsening of the Miocene tephra layers reflects more vigorous atmospheric circulation. Such conditions might lead to both increased grain size of individual layers and a higher frequency of layers. The past history of atmospheric circulation has been assessed in a semi-quantitative manner using the record of eolian components in deep-sea sediments (Rea, 1994). In particular, changes in the grain size of atmospherically transported dust has been used to make inferences about changes in the paleointensity of wind. These records predominantly reflect changes in tropospheric winds, as dust transport is restricted to such elevations. One of the best records of Cenozoic atmospheric circulation has been obtained from Core LL44-GPC3 from the central gyre region of the Pacific (Fig. 18). This core provides a nearly continuous record of dust transport that extends back 70 m.y. The most significant change in Cenozoic circulation occurred at the time of the Paleocene/Eocene boundary, when there was an abrupt reduction in the grain size of dust. This reduction has been attributed to a decrease in wind speed of a factor of three or four (Janecek and Rea, 1983). Throughout the Eocene the dust remained small but began to coarsen in the early Oligocene and then again during much of the middle Miocene. Continued coarsening is also associated with the onset of Northern Hemispheric glaciation in the late Pliocene. There does not appear

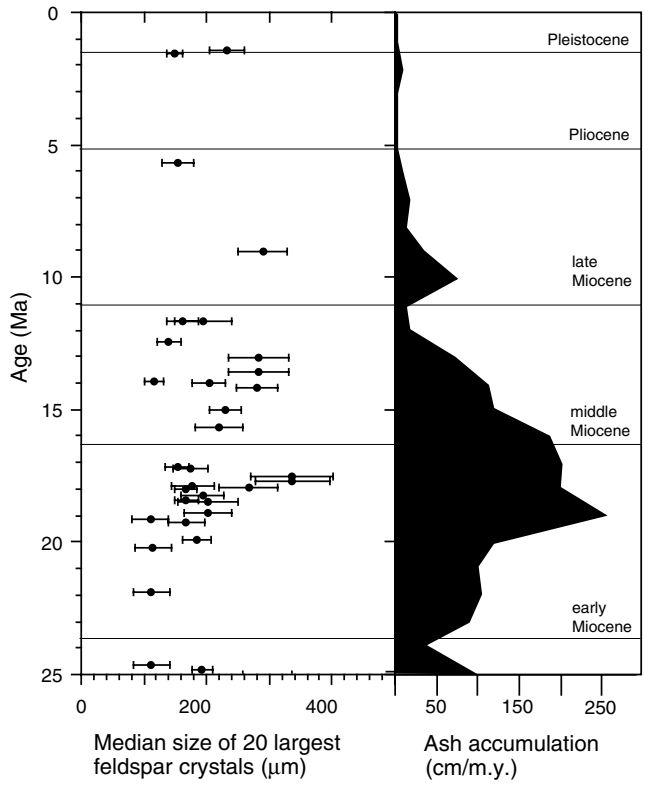

Figure 6. Variation in median size of the 20 largest feldspar crystals in tephra fall layers from Site 999 as a function of age (left). Also shown (right) is the record of total ash accumulation rate for Site 999 as a function of age (data from Sigurdsson, Leckie, Acton, et al., 1997).

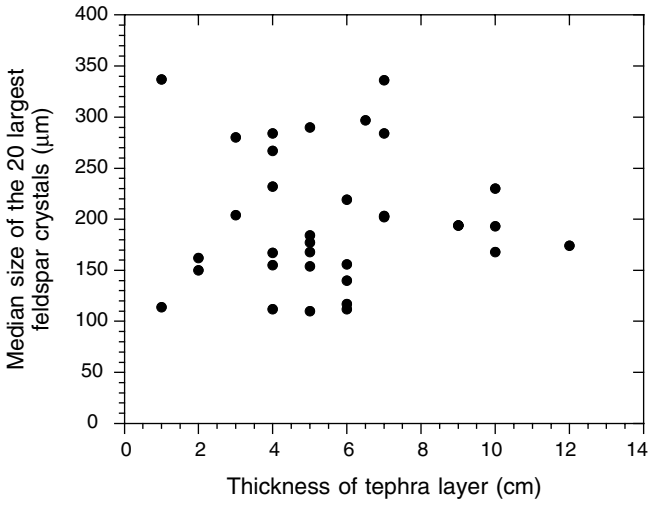

Figure 7. Variation in median size of the 20 largest feldspar crystals vs. thickness of tephra layer for Site 999.

to be any correlation between the western Caribbean Miocene peak in explosive volcanism and any distinct coarsening peak in the dust grain-size record (Fig. 18). The coarsest dust in the upper Cenozoic is actually deposited after the peak in explosive volcanism. Furthermore, there is also no correlation between the lower upper Eocene peak in explosive volcanism recorded at Site 999 and any significant coarsening in the dust record. This period corresponds to some of the finest grained dust deposition in the central Pacific.

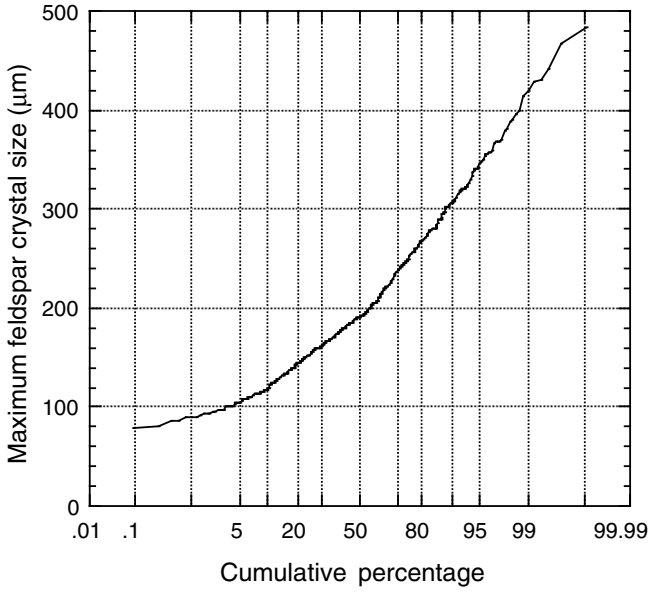

Figure 8. Cumulative percentage of maximum feldspar size in all measured Miocene tephra fall layers from Site 999.

The dust record of Core LL44-GPC3 provides information for winds at latitudes >20°N during its migration to the north on the Pacific plate and thus lies further north than the latitudinal belt associated with Caribbean tephra transport. There is evidence, however, that the current position of the boundary between the higher latitude westerlies and the lower latitude trade winds might have been different during the early Miocene. Rea (1994) has suggested that the decrease in grain size of the dust record from Core LL44-GPC3 in the lower Miocene may reflect passage of the site beneath a northerly displaced intertropical convergence zone (ITCZ) that was located at ~22°–24°N. The northward displacement of the ITCZ is attributed to an asymmetry of the thermal gradients between hemispheres, with the Southern Hemisphere exhibiting a strong gradient as a result of ice buildup on Antarctica and the Northern Hemisphere being characterized by warm and equitable climates with weaker thermal gradients. Under these conditions the boundary between the westerlies and trade winds in the northern hemisphere may have been somewhere between 40°N and 50°N (Rea, 1994). The southern trade winds would have been stronger during the early Miocene, owing to the higher pole-to-equator thermal gradient in the southern hemisphere. This configuration would be expected to enhance westerly transport of tephra from Central America as a result of low-level transport in the troposphere and perhaps diminish easterly transport into the Caribbean. However, the tephra record indicates the opposite, thus supporting the contention that the early to mid-Miocene peak in explosive volcanism is not a primary signal of major atmospheric circulation changes at that time.

We believe that the best explanation for the coarsening of the tephra layers is that eruption intensity, or column height, was greater for the event at the peak of the tephra accumulation episode. Eruption column height has a major impact on the dispersal of tephra because it defines the nature and extent of the umbrella region from which tephra is subsequently advected by prevailing winds (Sparks, 1986). The relationship between the dispersal area for a particular particle size and eruption column height is nonlinear, and, consequently, the variations in eruption column height can translate into large changes in dispersal efficiency (Carey and Sparks, 1986). Thus, the Miocene peak in explosive volcanism likely represented not only an increase in the frequency of eruptions but also an increase in the intensity of events, as reflected in higher eruption column heights.

Table 3. Feldspar size measurements of tephra fall layers, Site 1000.

Core, section	Layer (cm) Top	Base	Thickness	Age (Ma)	Size (μm) Median	Average	Standard deviation	Maximum	Minimum
165-1000B-									
16H-6	17	22	5	4.5	280	279	51	387	172
22H-2	53	61	8	6.5	200	211	33	273	151
27H-5	109	113	4	7.3	148	149	17	193	123
36X-1	76	78	2	9.6	148	149	17	193	123
40X-2	44	47	3	10.4	182	188	29	251	152
48X-4	143	145	2	12.6	155	161	28	221	121
53X-3	134	135	1	13.8	124	130	26	202	94
56X-3	51	53	2	14.6	276	285	35	356	247
4R-4	50	53	3	14.6	267	290	70	506	225
5R-2	33	34	1	14.8	260	270	54	418	197
7R-CC	0	6	6	15.5	416	434	86	678	344
11R-1	130	136	6	16.3	416	434	86	678	344
13R-5	94	101	7	17.0	170	179	32	280	142
14R-3	57	61	4	17.1	250	249	58	390	163
16R-4	73	104	31	17.7	580	575	105	728	377
16R-5	71	85	14	17.7	371	374	28	430	322
17R-4	14	17	3	17.9	352	371	55	468	291
18R-4	38	51	13	18.2	402	404	58	487	318
21R-4	19	72	53	19.0	373	362	53	442	247

Notes: Minimum size is of the 20 smallest feldspar crystals. All other measurements are of the 20 largest feldspar crystals. All measurements taken along the long axis.

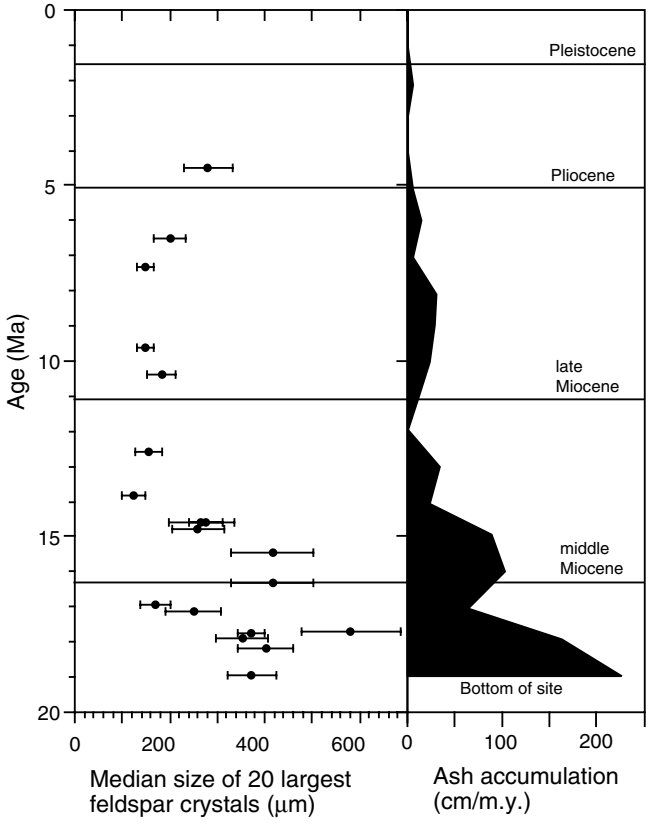

Figure 9. Variation in median size of the 20 largest feldspar crystals in tephra fall layers from Site 1000 as a function of age (left). Also shown (right) is the record of total ash accumulation rate for Site 1000 as a function of age (data from Sigurdsson, Leckie, Acton, et al., 1997).

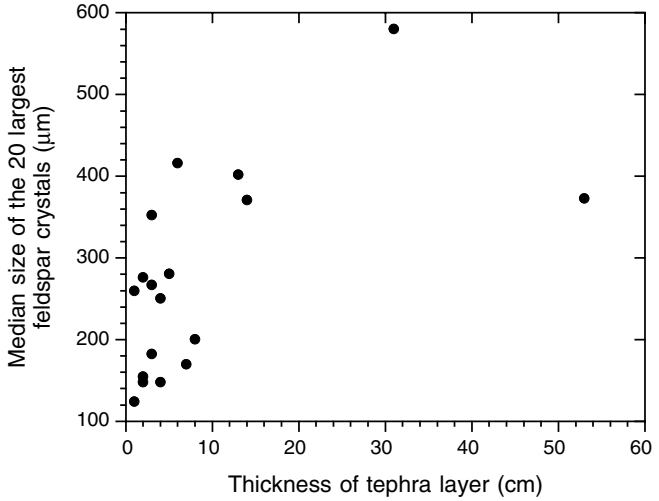

Figure 10. Variation in median size of the 20 largest feldspar crystals vs. thickness of tephra layer for Site 1000.

CONCLUSIONS

A combination of grain-size data from tephra layers in the western Caribbean (Sites 998, 999, and 1000) and consideration of the general atmospheric circulation of the area provides important insights into the location and nature of the source eruptions. Despite the dominance of easterly trade winds in the Caribbean area, a stronger westerly transport component is present at upper levels in the atmosphere, where tephra from explosive eruptions is typically injected. This component allows transport of material from Central American volcanism into the western Caribbean. The Lesser Antilles volcanic arc, located some 1500 km to the east, is too far away from Sites 998, 999, and 1000 to be a source for the abundant tephra layers given the circulation regime of the region and distribution of tephra layers in the eastern Caribbean and western equatorial Atlantic. Support for a western source comes from the abundance of dated Miocene pyroclastic deposits exposed throughout Central America.

Crystal sizes in the western Caribbean tephra layers suggest derivation from highly energetic explosive eruptions that generated voluminous pyroclastic flow and were associated with the formation of calderas. Based on comparisons with younger, well-documented marine tephra layers, many of the source eruptions for Leg 165 tephra layers were of the scale of the Campanian ignimbrite event that generated 80 km^3 of magma with an eruption column height of >40 km.

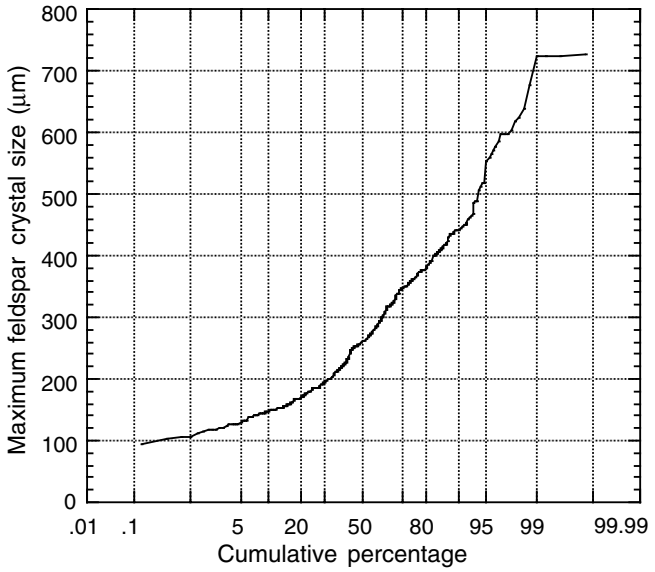

Figure 11. Cumulative percentage of maximum feldspar size in all measured Miocene tephra fall layers from Site 1000.

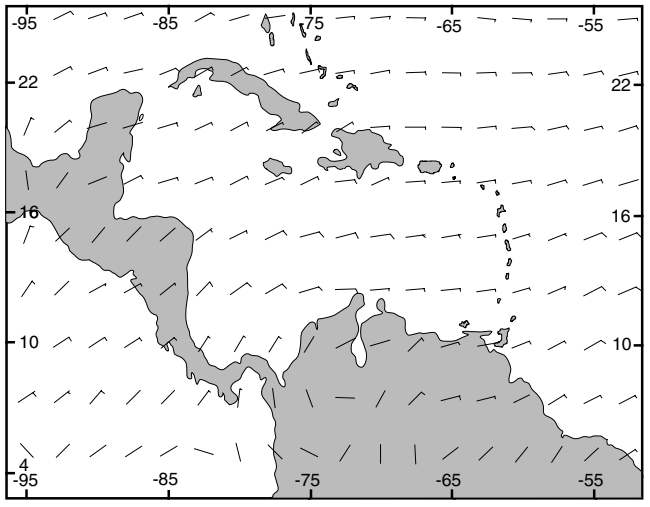

Figure 12. Vectors of surface winds (1000 mb level) in the Caribbean area. Each barb on the wind vector corresponds to a velocity of 5 m/s. Predominant transport at this level is from east to west in the trade winds. Source of data is the Global Upper Air Climatic Atlas (NOAA, 1993).

At all three sites there is a trend toward the coarsest crystal size to be associated with the early to mid-Miocene peak in explosive volcanism as defined by the accumulation rate per million years. This trend is not likely to be caused by paleowind variations during the last 20 m.y., as no significant correlation exists between the tephra grain-size record and the independent record of paleowind provided by eolian transport of material to the deep sea. We propose that the coarsening of the layers reflects the occurrence of higher intensity eruptions during the Miocene peak in explosive volcanism. Higher intensity eruption can greatly enhance the dispersal of tephra by generating high-altitude lateral injections of material that are then advected by the prevailing wind.

REFERENCES

Barberi, F., Innocenti, F., Lirer, L., Munro, R., Pescatore, T., and Santacroce, R., 1978. The Campanian ignimbrite: a major prehistoric eruption in the Neapolitan area (Italy). *Bull. Volcanol.*, 41:10–32.

Bursik, M.I., Sparks, R.S.J., Gilbert, J.S., and Carey, S.N., 1992. Sedimentation of tephra by volcanic plumes: I Theory and its comparison with a study of the Fogo A Plinian deposit, Sao Miguel (Azores). *Bull. Volcanol.,* 54:329–344.

Cadet, J.-P., Pouclet, A., Thisse, Y., Bardintzeff, J.M., and Azéma, J., 1982a. Middle America Neogene explosive volcanism and ash layers: evidence from the Middle America trench transect, Deep Sea Drilling Project Leg 167. *In* Aubouin, J., von Huene, R., et al., *Init. Repts. DSDP,* 67: Washington (U.S. Govt. Printing Office), 475–491. Cadet, J.-P., Thisse, Y., Pouclet, A., Bardintzeff, J.M., and Stephan, J.F., 1982b. Tephra from Deep Sea Drilling Project Leg 66: Middle American Trench Transect (Southern Mexico). *In* Watkins, J.S., Moore, J.C., et al., *Init. Repts. DSDP,* 66: Washington (U.S. Govt. Printing Office), 687–698.

Carey, S.N., 1996. Modeling of tephra fallout from explosive eruptions. *In* Scarpa, R., and Tilling, R. (Eds.), *Monitoring and mitigation of volcano hazards:* Berlin (Springer), 429–462.

Carey, S.N., and Sigurdsson, H., 1980. The Roseau ash: deep-sea tephra deposits from a major eruption on Dominica, Lesser Antilles Arc. *J. Volcanol. Geotherm. Res.*, 7:67–86.

————, 1982. Influence of particle aggregation on deposition of distal tephra from the May 18, 1980, eruption of Mount St. Helens volcano. *J. Geophys. Res.*, 87:7061–7072.

————, 1989. The intensity of Plinian eruptions. *Bull. Volcanol.*, 51:28–40.

Carey, S.N., and Sparks, R.S.J., 1986. Quantitative models of the fallout and dispersal of tephra from volcanic eruption columns. *Bull. Volcanol.*, 48:109–125.

Cashman, K., and Fiske, R., 1991. Fallout of pyroclastic debris from submarine volcanic eruptions. *Science*, 253:275–280.

Cornell, W., Carey, S., and Sigurdsson, H., 1983. Computer simulation of transport and deposition of the Campanian Y-5 ash. *J. Volcanol. Geotherm. Res.,* 17:89–109.

Drexler, J.W., Rose, W.I., Jr., Sparks, R.S.J., and Ledbetter, M.T., 1980. The Los Chocoyos ash, Guatemala: a major stratigraphic marker in middle America and three ocean basins. *Quat. Res.*, 13:327–345.

Ehrenborg, J., 1996. A new stratigraphy for the Tertiary volcanic rocks of the Nicaraguan Highland. *Geol. Soc. Am. Bull.*, 108:830–842.

Fisher, R.V., and Schmincke, H.-U., 1984. *Pyroclastic Rocks:* New York (Springer-Verlag).

Janecek, T.R., and Rea, D.K., 1983. Eolian deposition in the northeast Pacific Ocean: Cenozoic history of atmospheric circulation. *Geol. Soc. Am. Bull.,* 94:730–738.

Kennett, J.P., 1981. Marine tephrochronology. *In* Emiliani, C. (Ed.), *The Sea* (Vol. 7): *The Oceanic Lithosphere:* New York (Wiley), 1373–1436.

Ledbetter, M., 1985. Tephrochronology of marine tephra adjacent to Central America. *Geol. Soc. Am. Bull.*, 96:77–82.

McDowell, F.W., and Clabaugh, S.E., 1979. Ignimbrites of the Sierra Madre Occidental and their relation to the tectonic history of western Mexico. *Spec. Pap.—Geol. Soc. Am.,* 180:113–124.

Natland, J., 1984. Occurrences of air-fall volcanic ash derived from the Lesser Antilles arc at Leg 78A drill sites. *In* Biju-Duval, B., Moore, J.C., et al., *Init. Repts. DSDP,* 78 (Pt. 1): Washington (U.S. Govt. Printing Office), 369–375.

Ninkovich, D., Sparks, R.S.J., and Ledbetter, M.T., 1978. The exceptional magnitude and intensity of the Toba eruption, Sumatra: an example of the use of deep-sea tephra layers as a geological tool. *Bull. Volcanol.,* 41:286–297.

NOAA, 1993. *Global Upper Air Climatic Atlas,* ver. 1.0, vol. I, II [CD-ROM]. Available from: National Oceanic and Atmospheric Administration, National Climatic Data Center, Federal Building, 151 Patton Avenue, Asheville, NC 28801-5001, U.S.A.

Pyle, D.M., 1989. The thickness, volume and grain size of tephra fall deposits. *Bull. Volcanol.,* 51:1–15.

————, 1995. Assessment of the minimum volume of tephra fall deposits. *J. Volcanol. Geotherm. Res.,* 69:379–382.

Rea, D.K., 1994. The paleoclimatic record provided by eolian deposition in the deep sea: the geologic history of wind. *Rev. Geophys.,* 32:159–195.

Reynolds, J.H., 1980. Late Tertiary volcanic stratigraphy of northern Central America. *Bull. Volcanol.,* 43:601–607.

————, 1987. Timing and sources of Neogene and Quaternary volcanism in south-central Guatemala. *J. Volcanol. Geotherm. Res.*, 33:9–22.

Shipboard Scientific Party, 1997a. Site 998. *In* Sigurdsson, H., Leckie, R.M., Acton, G.D., et al., *Proc. ODP, Init. Repts*., 165: College Station, TX (Ocean Drilling Program), 49–130.

————, 1997b. Site 999. *In* Sigurdsson, H., Leckie, R.M., Acton, G.D., et al., *Proc. ODP, Init. Repts*., 165: College Station, TX (Ocean Drilling Program), 131–230.

————, 1997c. Site 1000. *In* Sigurdsson, H., Leckie, R.M., Acton, G.D., et al., *Proc. ODP, Init. Repts*., 165: College Station, TX (Ocean Drilling Program), 231–289.

Sigurdsson, H., and Carey, S., 1981. Marine tephrochronology and Quaternary explosive volcanism in the Lesser Antilles arc. *In* Self, S., and Sparks, R.S.J. (Eds.), *Tephra Studies*: London (D. Reidel), 255–280.

Sigurdsson, H., Leckie, R.M., Acton, G.D., et al., 1997. *Proc. ODP, Init. Repts.,* 165: College Station, TX (Ocean Drilling Program).

Sigurdsson, H., Sparks, R.S.J., Carey, S.N., and Huang, T.C., 1980. Volcanogenic sedimentation in the Lesser Antilles arc. *J. Geol.,* 88:523–540.

Sparks, R.S.J., 1986. The dimensions and dynamics of volcanic eruption columns. *Bull. Volcanol.*, 48:3–15.

Sparks, R.S.J., Bursik, M., Carey, S., Gilbert, J., Glaze, L., Sigurdsson, H., and Woods, A., 1997. *Volcanic Plumes:* Chichester (J. Wiley and Sons).

Sparks, R.S.J., Carey, S., and Sigurdsson, H., 1991. Sedimentation from gravity currents generated by turbulent plumes. *Sedimentology,* 38:839–856.

Sparks, R.S.J., and Huang, T.C., 1980. The volcanological significance of deep-sea ash layers associated with ignimbrites. *Geol. Mag.*, 117:425–436.

Watkins, N.D., Sparks, R.S.J., Sigurdsson, H., Huang, T.C., Federman, A., Carey, S., and Ninkovich, D., 1978. Volume and extent of the Minoan tephra layer from Santorini volcano: new evidence from deep-sea sediment cores. *Nature,* 271:122–126.

Wiesemann, G., 1975. Remarks on the geologic structure of the Republic of El Salvador. *Mitt. Geol.-Palaeontol. Inst. Univ. Hamburg,* 44:557–574.

Wilson, L., and Huang, T.C., 1979. The influence of shape on the atmospheric settling velocity of volcanic ash particles. *Earth Planet. Sci. Lett.*, 44:311–324.

Woods, A.W., and Wohletz, K., 1991. Dimensions and dynamics of co-ignimbrite eruption columns. *Nature,* 350:225–227.

Date of initial receipt: 24 June 1998
Date of acceptance: 8 February 1999
Ms 165SR-002

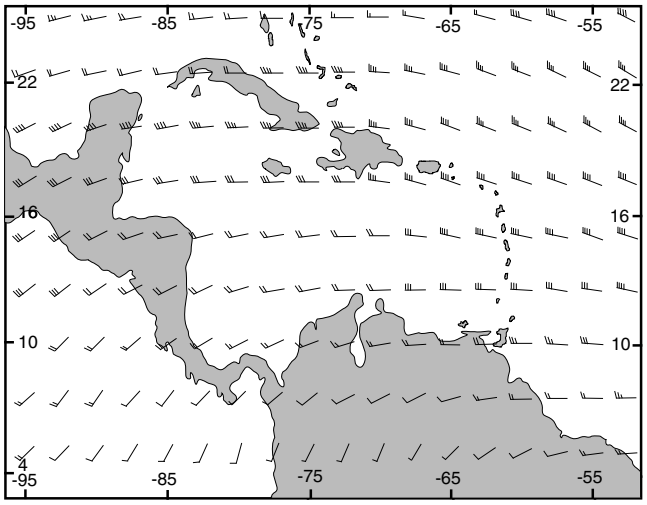

Figure 13. Vectors of upper level winds (750 mb level, 11 km height) in the Caribbean area. Each barb on the wind vector corresponds to a velocity of 5 m/s. Predominant transport at this level is from west to east. Source of data is the Global Upper Air Climatic Atlas (NOAA, 1993).

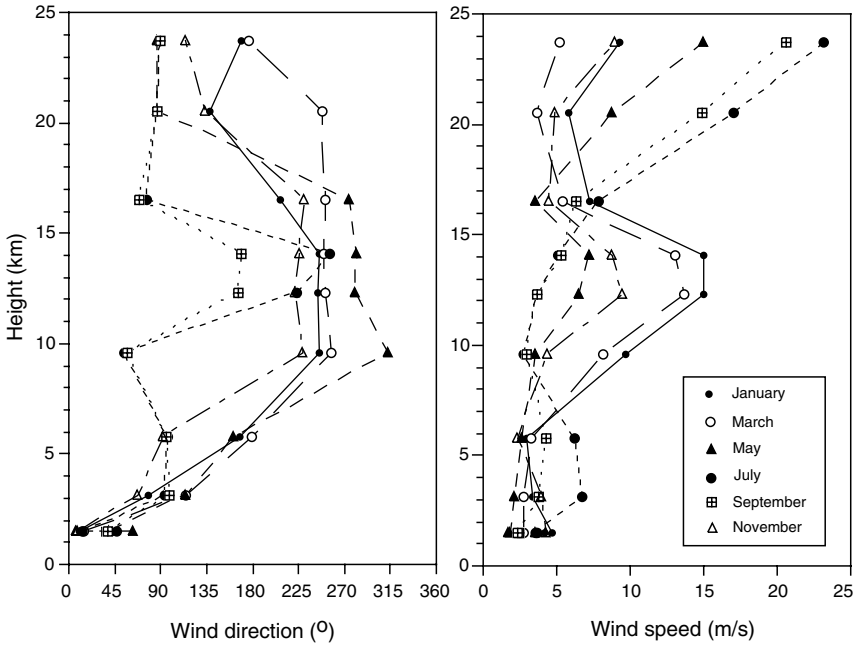

Figure 14. Variation in wind direction (left) and velocity (right) as a function of altitude at Guatemala City, Guatemala. Note the seasonal variability in both direction and velocity. Source of data is the Global Upper Air Climatic Atlas (NOAA, 1993).

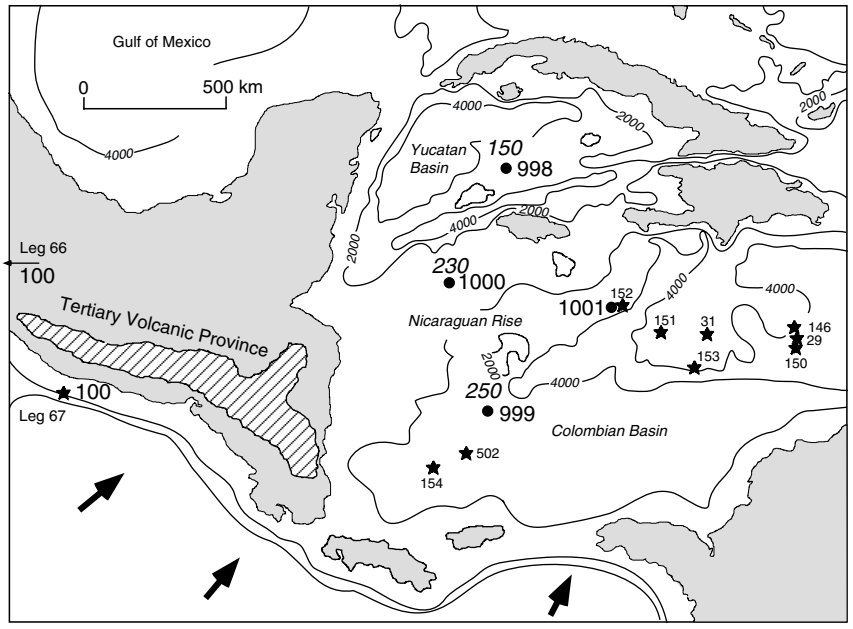

Figure 15. Reconstruction of the Caribbean area during the mid-Miocene showing the location of Leg 165 (solid circles) and other DSDP/ODP sites (stars) (Sigurdsson, Leckie, Acton, et al., 1997). Italicized numbers next to the Leg 165 sites indicate the peak accumulation rate in centimeters per million years of volcanic ash during the Miocene.

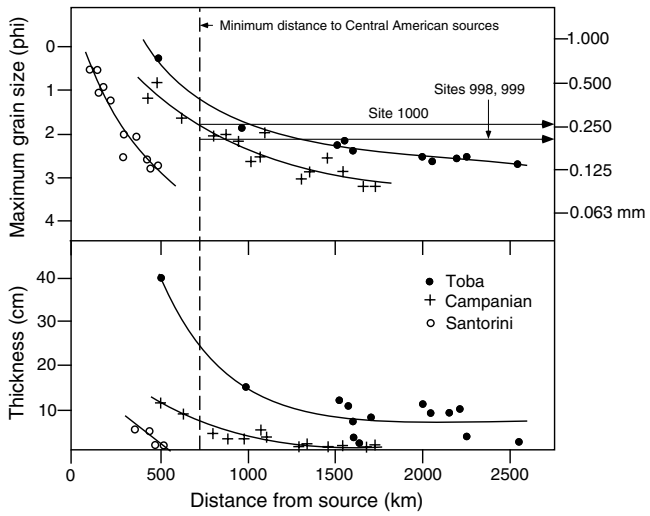

Figure 16. Variation in maximum grain size and thickness for the Toba, Campanian, and Santorini marine tephra fall layers (from Fisher and Schmincke, 1984). Vertical dashed line corresponds to the minimum distance from the Central American Tertiary volcanic province to Leg 165 Sites 998, 999, and 1000. Horizontal lines with arrows show the mean of the maximum feldspar crystal sizes in the Miocene tephra layers from Sites 998, 999, and 1000.

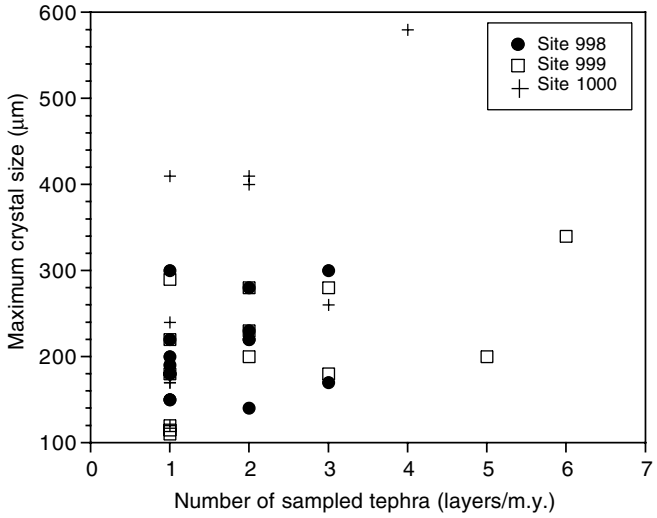

Figure 17. Comparison of the maximum feldspar crystal size found in tephra fall layers vs. the number of tephra layers sampled in a 1-m.y. interval for Sites 998, 999, and 1000.

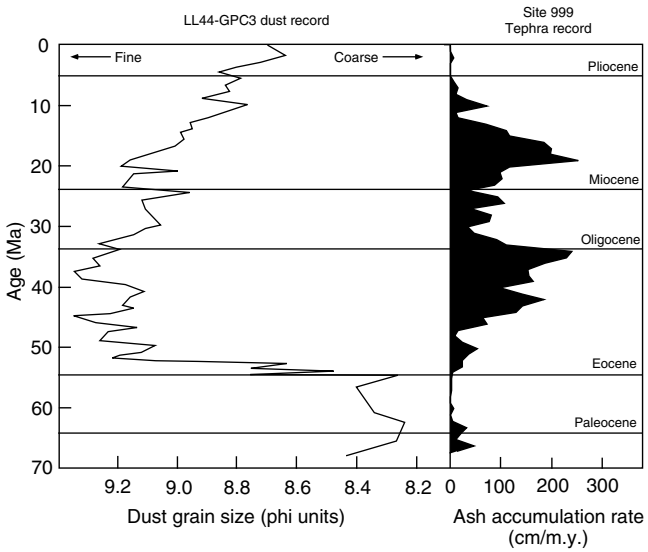

Figure 18. Comparison of the ash accumulation rate at Site 999 (right) with the dust grain-size record of Core LL44-GPC3 in the central Pacific. Ash accumulation data from Sigurdsson, Leckie, Acton, et al. (1997) and dust grain size from Rea (1994).